

Modulation of the molecular composition of large conductance, Ca²⁺ activated K⁺ channels in vascular smooth muscle during hypertension

See the related Commentary beginning on page 654.

Gregory C. Amberg,¹ Adrian D. Bonev,² Charles F. Rossow,¹ Mark T. Nelson,² and Luis F. Santana¹

¹Department of Physiology and Biophysics, University of Washington, Seattle, Washington, USA

²Department of Pharmacology, The University of Vermont College of Medicine, Burlington, Vermont, USA

Hypertension is a clinical syndrome characterized by increased vascular tone. However, the molecular mechanisms underlying vascular dysfunction during acquired hypertension remain unresolved. Localized intracellular Ca²⁺ release events through ryanodine receptors (Ca²⁺ sparks) in the sarcoplasmic reticulum are tightly coupled to the activation of large-conductance, Ca²⁺-activated K⁺ (BK) channels to provide a hyperpolarizing influence that opposes vasoconstriction. In this study we tested the hypothesis that a reduction in Ca²⁺ spark–BK channel coupling underlies vascular smooth muscle dysfunction during acquired hypertension. We found that in hypertension, expression of the β1 subunit was decreased relative to the pore-forming α subunit of the BK channel. Consequently, the BK channels were functionally uncoupled from Ca²⁺ sparks. Consistent with this, the contribution of BK channels to vascular tone was reduced during hypertension. We conclude that downregulation of the β1 subunit of the BK channel contributes to vascular dysfunction in hypertension. These results support the novel concept that changes in BK channel subunit composition regulate arterial smooth muscle function.

J. Clin. Invest. 112:717–724 (2003). doi:10.1172/JCI200318684.

Introduction

Chronic hypertension increases morbidity and mortality from stroke, coronary artery disease, congestive heart failure, and renal disease (1, 2). Sustained increases in arterial tone are an essential component in the development of hypertension (3, 4). Mounting evidence suggests that sustained depolarization (5, 6) of smooth muscle underlies the increase in arterial tone during hypertension by increasing the open probability of voltage-dependent L-type Ca²⁺ channels (6). The resulting increase in Ca²⁺ influx raises global intracellular Ca²⁺ ([Ca²⁺]_i) and contributes to constriction (7, 8). The molecular mechanisms underlying these changes in vascular smooth muscle function during hypertension are presently unclear.

Unlike a global elevation of [Ca²⁺]_i, highly localized intracellular Ca²⁺ transients (Ca²⁺ sparks), originating

from ryanodine-sensitive Ca²⁺-release channels (ryanodine receptors [RyRs]) in the sarcoplasmic reticulum (SR), increase [Ca²⁺]_i locally but do not cause contraction (9). Instead, Ca²⁺ sparks oppose depolarizing contractile stimuli by activating closely apposed, large-conductance, Ca²⁺-activated K⁺ (BK) channels (9, 10). An important implication of this model is that dynamic regulation of BK channel activity by Ca²⁺ sparks may be critical in the determination of vascular tone and blood pressure. Consistent with this, vasoconstrictors, acting through stimulation of PKC, decrease BK channel activity indirectly by inhibiting Ca²⁺ sparks (11). Conversely, increasing Ca²⁺ spark activity through cAMP-dependent signaling or enhancing BK channel coupling to Ca²⁺ sparks causes vasodilation (12, 13). These studies suggest a central role for RyR–BK channel communication via local Ca²⁺ signals in the regulation of arterial tone and blood pressure.

BK channels in vascular smooth muscle are composed of pore-forming α and accessory β1 subunits (14, 15). Coexpression of the β1 subunit results in BK channels with increased Ca²⁺ sensitivity (16, 17). The β1 subunit appears to be uniquely expressed in smooth muscle (18). A functional role for the β1 subunit in vascular smooth muscle was recently demonstrated in genetically engineered mice lacking expression of this subunit (18–20). These studies showed that targeted deletion of the β1 subunit uncoupled BK channels from Ca²⁺ sparks, and thereby decreased the contribution of BK channels to the

Received for publication April 17, 2003, and accepted in revised form May 27, 2003.

Address correspondence to: L.F. Santana, Department of Physiology and Biophysics, University of Washington, Box 357290, Seattle, Washington 98195, USA. Phone: (206) 543-0986; Fax: (206) 685-0619; E-mail: santana@u.washington.edu.

Conflict of interest: The authors have declared that no conflict of interest exists.

Nonstandard abbreviations used: Ca²⁺-activated K⁺ (BK); global intracellular Ca²⁺ ([Ca²⁺]_i); ryanodine receptor (RyR); sarcoplasmic reticulum (SR); hypertensive (HT); normotensive (NT); hydroxyethylenediaminetetraacetic acid (HEDTA); open channel probability (P_o); bicarbonate-based PSS (B-PSS); ibertioxin (Ibtx); holding potential (HP); tamoxifen (Tam); spontaneously hypertensive rats (SHR); Wistar Kyoto rats (WKY).

regulation of vascular tone. Importantly, $\beta 1$ KO mice were hypertensive (HT), indicating that uncoupling BK channels from RyRs by the loss of the $\beta 1$ subunit alone is sufficient to induce hypertension.

$\beta 1$ subunit expression is high in arteries from normotensive (NT) animals (18–20). Consequently, in NT arteries, RyR-BK channel coupling is strong (10). It is unclear, however, whether a disruption of RyR-BK channel communication is involved in the progression from a NT to a HT state. Because proper RyR-BK channel communication is important for normal arterial function, we tested the hypothesis that during hypertension, downregulation of the $\beta 1$ subunit results in BK channels with a diminished capacity to regulate vascular tone. We found that during Ang II-induced hypertension, BK channels were less sensitive to activation by Ca^{2+} sparks and were less able to regulate vascular tone. In agreement with these observations, we detected a decrease in the expression of the $\beta 1$ subunit; expression of the α subunit was unchanged. From these observations, we conclude that downregulation of the $\beta 1$ subunit of the BK channel contributes to vascular dysfunction during hypertension.

Methods

Ang II infusion and blood pressure measurements. Male Sprague-Dawley rats (250 g) were made HT by subcutaneous implantation of osmotic minipumps (Alzet, Durect Corporation, Cupertino, California, USA) delivering Ang II (250 ng/kg/day). Consistent with previous reports (21), 7 days after pump implantation the systolic blood pressure of Ang II-infused rats increased from 120 ± 4 mmHg to 213 ± 7 mmHg ($P < 0.05$, $n = 9$). Over the same period, sham-operated controls did not experience changes in systolic blood pressure (120 ± 2 mmHg vs. 124 ± 4 mmHg, $P > 0.05$, $n = 8$). Blood pressure measurements were taken with a tail-cuff plethysmograph from Narco Bio-Systems (Houston, Texas, USA) as previously described (21). Animals were handled in strict accordance to the guidelines of the University of Washington Institutional Animal Care and Use Committee.

Isolation of vascular myocytes. Rats were killed with a lethal dose of sodium pentobarbital (100 mg/kg intraperitoneally) as approved by the University of Washington Institutional Animal Care and Use Committee. Smooth muscle cells were prepared from basilar, posterior, and midcerebral arteries using standard enzymatic dissociation methods (10).

Electrophysiology. BK currents were measured with the whole-cell patch clamp technique in the amphotericin B (250 $\mu\text{g}/\text{ml}$) perforated-patch configuration with the use of an Axopatch 200B amplifier (Axon Instruments Inc., Union City, California, USA). During experiments, cells were continuously superfused with a normal Tyrode's solution with the following constituents: 130 mM NaCl, 5 mM KCl, 2 mM CaCl_2 , 1 mM MgCl_2 , 10 mM glucose, and 10 mM HEPES (pH = 7.4). Patch pipettes were filled with a solution composed of the

following: 110 mM K-aspartate, 30 mM KCl, 10 mM NaCl, 1 mM MgCl_2 , 0.5 mM EGTA, and 10 mM HEPES (pH = 7.3). Spontaneous, transient outward currents resulting from the concerted opening of a few BK channels were analyzed with Mini-Analysis software (Synsoft Inc., Decatur, Georgia, USA).

For single-channel experiments, currents were digitized at 5 kHz using pCLAMP 8 software (Axon Instruments Inc.). Single-channel records were filtered at 1 kHz with a Bessel filter (8 pole). Smooth muscle cells were bathed in a solution containing: 140 mM KCl, 1 mM EGTA or 1 mM hydroxyethylenediaminetetraacetic acid (HEDTA), and 10 mM HEPES, adjusted to pH 7.3 with Tris. Ca^{2+} (CaCl_2) was added to achieve the desired level of free Ca^{2+} (determined using WinMAXC software; C. Patton, Stanford University Pacific Grove, California, USA; <http://www.stanford.edu/~cpatton/maxc.html>). Pipettes were filled with the same 140 mM K^+ solution without Ca^{2+} supplementation. BK channel currents were recorded from inside-out patches under symmetrical (140 mM) K^+ . Data were analyzed with pClamp 8 (Axon Instruments Inc.) and the Analysis of Single Channel Data software (University of Leuven, Leuven, Belgium). BK channel number, conductance, and open probability (P_o) were determined from all-points amplitude histograms; only recordings with stable P_o values for a minimum 2 minutes were analyzed. The number of BK channels per patch was estimated while patches were held at +80 mV in the presence of 10^{-5} Ca^{2+} , which maximizes the P_o of these channels (17).

$[\text{Ca}^{2+}]_i$ imaging. Imaging of Ca^{2+} sparks was performed on cells loaded with the fluorescent Ca^{2+} indicator fluo-4-AM (10) (50 μM) using a Radiance 2100 confocal system (Bio-Rad Laboratories Inc., Hercules, California, USA), coupled to a Nikon TE300 inverted microscope using a Nikon 60X water immersion lens (numerical aperture = 1.2) (Nikon Inc., Melville, New York, USA). Images were analyzed with custom software written in IDL language (Research Systems Inc., Boulder, Colorado, USA). Ca^{2+} sparks were identified with a computer algorithm similar to the one described by Cheng et al. (22). Images were normalized by dividing the fluorescence intensity of each pixel (F) by the average resting fluorescence intensity (F_0) of a confocal image to generate an F/F_0 image.

Intact artery measurements. Measurements of the diameter of intact pressurized arterial segments were performed as previously described (18). Briefly, arteries cleaned from connective tissue were cannulated and mounted in a close-working-distance arteriograph. The arteriograph was then mounted on the stage of an inverted microscope. After mounting the arteriograph, superfusion (3–6 ml/min) of a bicarbonate-based PSS (B-PSS) at 37°C began immediately. The B-PSS contained: 119 mM NaCl, 4.7 mM KCl, 24 mM NaHCO_3 , 1.2 mM KH_2PO_4 , 1.6 mM CaCl_2 , 1.2 mM MgSO_4 , 0.023 mM EDTA, and 11 mM glucose. The pH of this solution was set to 7.4 by bubbling with a gas mixture of O_2 (95%) and CO_2 (5%). After equilibration (≈ 20 minutes),

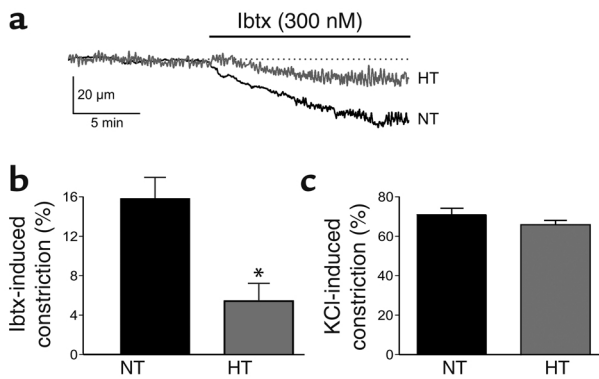


Figure 1

HT cerebral arteries are less sensitive to Ibtx than NT cerebral arteries. (a) Representative arterial diameter records from pressurized (60 mmHg) NT (black) and HT (red) arteries before and after the application of Ibtx (300 nM). Before the addition of Ibtx, the diameter of the HT and NT pressurized arteries were, respectively, 87 μm (passive diameter = 146 μm) and 130 μm (passive diameter = 148 μm). (b) Mean ± SEM of Ibtx-induced constriction in NT and HT arteries. (c) Mean ± SEM of KCl-induced (60 mM) constriction in NT and HT arteries. * $P < 0.05$.

intravascular pressure was increased to the physiologic level of 60 mmHg. Arterial diameters were measured from live video images with the length-calibrated edge-detection function of IonOptix imaging software (IonOptix, Milton Massachusetts, USA) at a sampling rate of 2 Hz. Experiments started after a stable level of tone was obtained. A constriction in response to iberitoxin (Ibtx) or KCl is presented as percentage constriction. The percentage constriction was obtained by dividing the arterial diameter after the stable development of tone by the diameter of the artery in the presence of a diltiazem (30 μM)-containing, Ca^{2+} -free (with 1 mM EGTA) B-PSS (passive diameter) and multiplying the number by 100. Addition of papaverine (100 μM) to this solution did not produce further constriction of NT or HT arteries ($n = 3$ each; data not shown).

RNA isolation and RT-PCR. Total RNA was isolated from rat cerebral arteries using the TRIzol reagent (Invitrogen, Carlsbad, California, USA) as per the manufacturer's protocol. Reverse transcription was performed using the Superscript First-strand Synthesis system (Invitrogen) with random primers according to the manufacturer's instructions. Primers specific to α (GenBank accession no. NM 031828; sense NT 1000-1021 and antisense NT 1180-1199, amplicon = 200 bp), $\beta 1$ (GenBank accession no. NM 019273; sense NT 494-513 and antisense NT 721-742, amplicon = 249), and β -actin (GenBank accession no. V01217; sense NT 2384-2404 and antisense NT 3071-3091, amplicon = 496 bp) were designed to identify the presence of each transcript in cerebral arterial vascular smooth muscle. The β -actin primers were designed to amplify a region between exons 4 and 6 such that genomic contamination within the RNA preparation could be identified by the presence of a 708-bp band in addition to the 496-bp band corresponding to the β -actin

transcript. PCR was performed with PCR Supermix (Invitrogen). After initial denaturation for 3 minutes at 94°C, samples underwent an additional 25 cycles at 94°C for 30 seconds, 52°C for 30 seconds, and 72°C for 1:30 seconds, followed by a final extension step at 72°C for 7 minutes. Amplicons were visualized using 2% agarose gel electrophoresis.

Real-time RT-PCR. Real-time RT-PCR was performed with the TaqMan 5' nuclease assay on an ABI Prism 7700 (Applied Biosystems, Foster City, California, USA) with the TaqMan Onestep PCR Mastermix (Applied Biosystems) using gene-specific primers during RT-PCR. Briefly, a standard curve was generated for each set of primers and probes with the use of \log_{10} serial dilutions. Standard curves were generated during each real-time RT-PCR session and were used to determine the relative abundance of α and $\beta 1$ transcripts. These values were normalized to endogenous 18S ribosomal RNA within the same sample. The slopes of our standard curves for α , $\beta 1$, and 18S were similar (-3.5 ± 0.1 Ct / [mRNA]; $n = 6$; $r^2 = 0.997-0.999$ in all cases). Thus, the efficiency of our primer and probe sets was considered equal and permitted relative quantitation and comparison of α and β transcripts. Primers and probes for real-time RT-PCR were as follows: α (GenBank accession no. NM 031828) sense NT 4100-4123, antisense NT 4157-4172, and probe NT 4134-4155; and $\beta 1$ (GenBank accession no. NM 019273) sense NT 683-708, antisense NT 740-762, and probe NT 710-732. 20x pre-developed TaqMan assay reagent for 18s ribosomal RNA was obtained from Applied Biosystems. After reverse transcription at 48°C for 30 minutes, AmpliTaq polymerase was activated at 95°C for 10 minutes, samples underwent 40 cycles of amplification in which they were incubated at 95°C for 15 seconds and 60°C for 1 minute. Samples ($n = 3$ for each tissue) were run in triplicate; RT(-) and nontemplate controls were included as a control for nonspecific amplification.

Statistics. Data are presented as mean ± SEM. Two-group comparisons were made using a Student *t* test. A *P* value of less than 0.05 was used as an indicator of significance. The asterisk (*) symbol is used in the figures to illustrate a significant difference between groups.

Results

Ibtx causes smaller constrictions in HT than NT cerebral arteries. Our first series of experiments examined the functional contribution of BK channel activity to vascular tone in pressurized (60 mmHg) cerebral arteries from NT control (systolic pressure = 124 ± 4 mmHg) and HT rats (systolic pressure = 213 ± 7 mmHg; Figure 1). As shown previously (23, 24), the BK channel-specific inhibitor Ibtx (300 nM) (25) caused a robust constriction of pressurized arteries from NT controls ($16\% \pm 2\%$; $n = 5$ arteries), which is consistent with BK channel activity opposing vasoconstriction. In contrast, pressurized arteries from HT animals constricted weakly to Ibtx ($5\% \pm 2\%$; $P < 0.05$, $n = 5$ arteries). To test that the diminished capacity of HT arteries to

constrict to Ibtx did not reflect an inability of these arteries to constrict, we examined the effects of 60 mM KCl on NT and HT vascular tone. We found that 60 mM KCl evoked significant constrictions of equal magnitude ($P < 0.05$) in NT ($70.8\% \pm 3.3\%$; $n = 5$) and HT ($65.6\% \pm 1.8\%$; $n = 5$) (Figure 1c). These data indicate that the weak constrictions induced by Ibtx in HT arteries were not due to these arteries being unable to respond to contractile stimuli. Taken together, our data support the hypothesis that decreased BK channel activity occurs during hypertension.

Uncoupling of Ca^{2+} sparks and BK channels in HT arterial myocytes. One possible mechanism for reducing BK channel activity in HT arteries is a decrease in smooth muscle Ca^{2+} spark activity. Therefore, we examined Ca^{2+} sparks and BK currents in isolated cerebral arterial smooth muscle cells. Figure 2a illustrates representative line-scan confocal images of Ca^{2+} sparks from NT and HT myocytes. The rates of spontaneous Ca^{2+} sparks were similar in NT and HT cells (3.07 ± 0.18 Hz, $n = 6$ vs. 3.03 ± 0.16 Hz, $n = 6$; $P > 0.05$) in voltage-clamped myocytes (holding potential = -40 mV). Interestingly, the amplitude of Ca^{2+} sparks in HT cells was larger than in NT cells ($1.63 \pm 0.01 F/F_0$, $n = 707$ vs. $1.71 \pm 0.01 F/F_0$, $n = 668$; $P < 0.05$). In addition, Ca^{2+} sparks in HT cells decayed slower than in NT cells; the average time for a Ca^{2+} spark to decay to 50% of its amplitude in HT and NT cells was 91.1 ± 3.9 ms and 63.9 ± 3.18 ms, respectively ($P < 0.05$, $n = 75$). These

data show that a decrease in Ca^{2+} spark activity cannot account for the decreased BK channel activity observed in HT arteries.

We therefore considered the alternative hypothesis that the efficiency with which Ca^{2+} sparks activate BK currents is diminished during hypertension. To test this, we performed simultaneous measurements of Ca^{2+} sparks and BK currents in control and HT cerebral arterial myocytes (Figure 2b). Measurements were performed at the physiologic holding potential (HP) of -40 mV (8) using the whole-cell patch clamp technique in the perforated-patch configuration. In agreement with previous work (10), Ca^{2+} spark and BK current amplitudes were highly correlated in NT arterial smooth muscle cells. However, note that in HT cells, Ca^{2+} sparks of similar amplitude to those observed in NT cells evoked smaller BK currents (Figure 2c). Indeed, the mean transient BK current amplitude for a given Ca^{2+} spark was approximately 50% lower in HT cells than in control cells (Figure 2d). Interestingly, the duration of BK currents at 50% of their amplitude was similar in HT (20.29 ± 1.00 ms) and NT (21.54 ± 1.02 ms) cells ($P > 0.05$, $n = 100$).

It is possible that a reduction in the number of functional BK channels could underlie the smaller BK currents observed in HT myocytes. However, we found that the number of BK channels in excised (inside-out) membrane patches from NT ($n = 12$) and HT ($n = 15$) myocytes was similar (about 3 channels per patch, $P > 0.05$; Figure 3d). In addition, the unitary conductance of BK channels

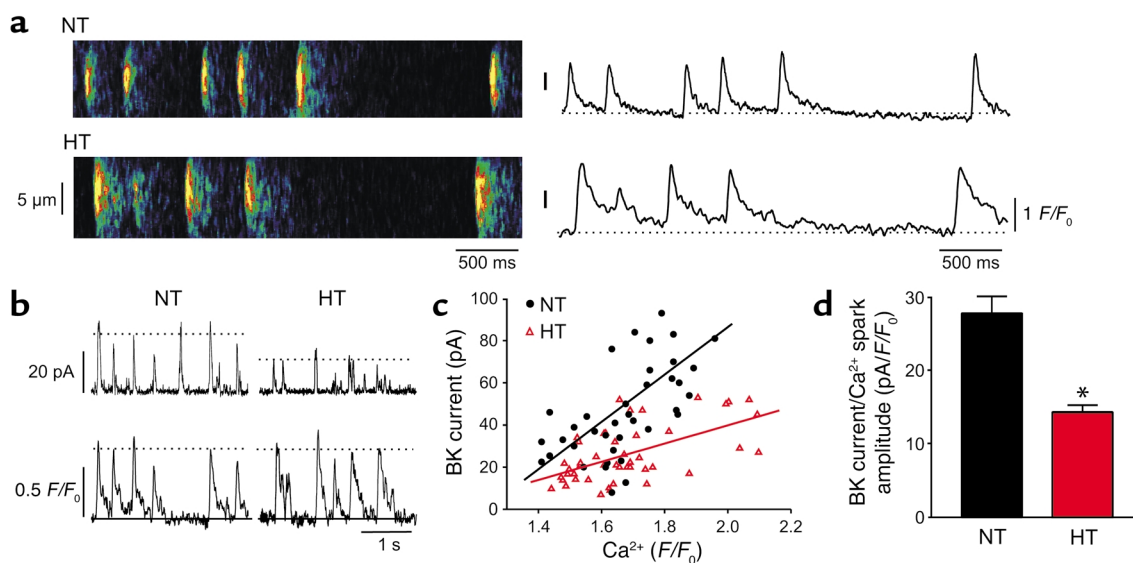


Figure 2

Reduced coupling between Ca^{2+} sparks and BK channels in HT arterial myocytes. (a) Representative line-scan images of Ca^{2+} sparks from NT and HT myocytes (left side). The traces to the right show the time course of $[Ca^{2+}]_i$ in the regions of the images delimited by the bars located at the end of each line-scan image. (b) Simultaneous BK current (top; HP = -40 mV) and Ca^{2+} sparks (bottom) recordings from NT and HT myocytes. In all cases, Ca^{2+} sparks had an associated BK current. However, on occasion, a Ca^{2+} spark outside the imaged area would evoke a BK current (e.g., the fifth BK current from left in NT cell). Dashed lines indicate the mean pA or F/F_0 (as appropriate) for each representative trace. (c) Relationship between BK current and Ca^{2+} spark amplitudes in NT (circles; 46 sparks from 6 cells) and HT (triangles; 41 sparks from 6 cells) myocytes. Data for this plot were obtained from traces similar to those shown in b. The smooth lines represent the best linear regression fits using a least-squares routine. The slope of the line used to fit the NT and HT data was, respectively, 112.4 ± 26.8 and 43.2 ± 9.2 pA/ Ca^{2+} (F/F_0). (d) Coupling strength (BK current amplitude divided by Ca^{2+} spark amplitude) in NT and HT myocytes. * $P < 0.05$.

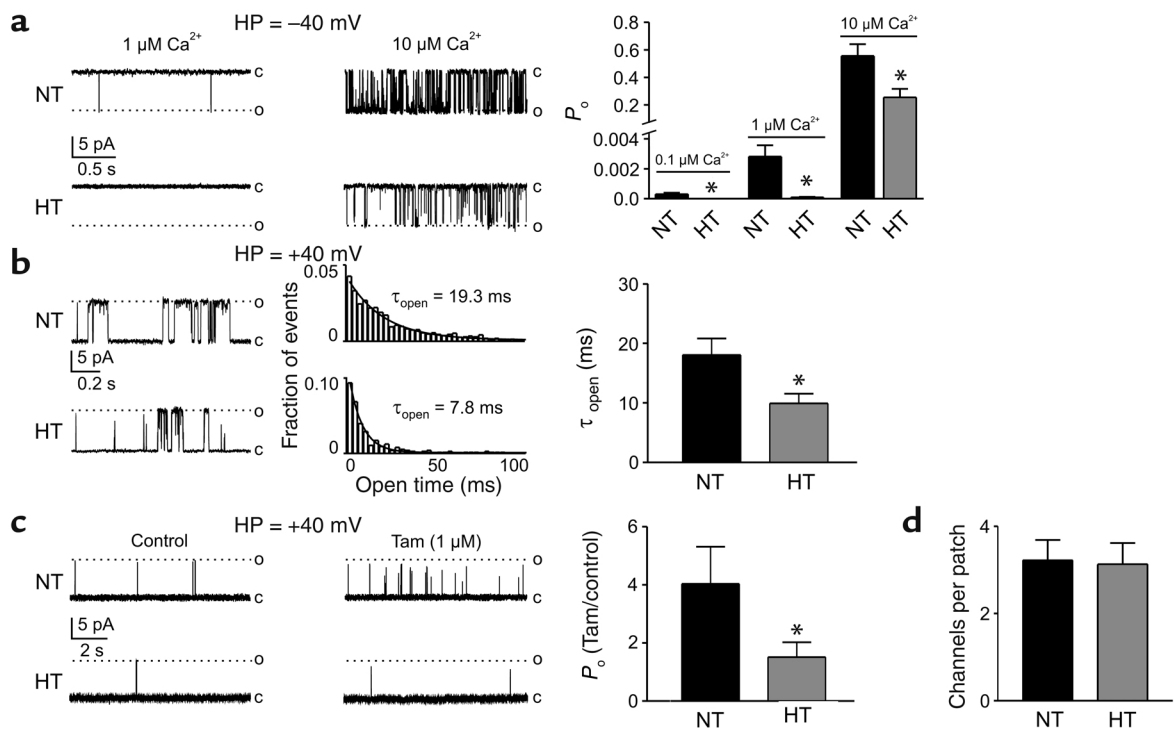


Figure 3

Functional and pharmacologic properties of single BK channels indicate decreased $\beta 1$ subunit function in HT myocytes. (a) Ca^{2+} sensitivity of BK channels in inside-out patches (HP = -40 mV) from NT and HT myocytes. Shown to the left are representative single BK channel records taken from NT and HT patches in the presence of 1 or $10 \mu\text{M}$ Ca^{2+} . The bar plot to the right shows the mean \pm SEM P_o of BK channels in NT and HT patches at three Ca^{2+} concentrations. (b) Open-time analysis of BK channels in inside-out patches from NT and HT myocytes. Shown to the left are representative single BK channel records taken from NT and HT patches at $+40$ mV in the presence of $1 \mu\text{M}$ Ca^{2+} . The open-time histograms of these BK channels from NT and HT myocytes are shown in the center. Histograms were fitted with a single exponential function. The bar plot to the right shows the mean \pm SEM τ_{open} of BK channels in NT and HT cells. (c) Tam ($1 \mu\text{M}$) sensitivity of BK channels in inside-out patches (HP = $+40$ mV; 100 nM free Ca^{2+}) from NT and HT myocytes. Shown to the left are representative single BK channel records taken from NT and HT patches before and after the application of Tam. The bar plot to the right shows the mean \pm SEM fold change in the P_o of BK channels in NT and HT cells after the application of Tam. (d) Number of BK channels per patch. Dashed lines indicate open channels. o, open channel; c, closed channel. $*P < 0.05$.

(symmetrical 140 mM K^+) in NT and HT cells was not different (265 ± 6 picosiemens, $n = 5$, vs. 268 ± 1 picosiemens, $n = 5$; $P > 0.05$). Thus, the smaller BK current amplitudes observed in HT myocytes results from reduced coupling efficiency between Ca^{2+} sparks and BK channels.

Decreased $\beta 1$ subunit function in HT myocytes. One plausible mechanism for reduced coupling efficiency is a decrease in the sensitivity of BK channels to activation by Ca^{2+} . Therefore, we compared the apparent Ca^{2+} sensitivity of BK channels in excised patches from NT and HT myocytes. In these experiments we exposed the intracellular aspect of the BK channels to Ca^{2+} concentrations of 0.1 , 1 , and $10 \mu\text{M}$ (HP = -40 mV). Figure 3a shows that at the three Ca^{2+} levels examined, the P_o of BK channels from HT cells was smaller than that of channels from NT cells ($P < 0.05$, $n = 8$ patches each). Indeed, at $10 \mu\text{M}$ Ca^{2+} , the P_o of BK channels from HT cells was about 50% smaller than in NT cells.

The pore-forming α subunit of the BK channel possesses intrinsic sensitivity to activation by Ca^{2+} (26). However, the Ca^{2+} sensitivity of these channels is enhanced by the presence of accessory β subunits

(27–29). Cerebral arterial smooth muscle cells of $\beta 1$ KO mice have BK channels with reduced Ca^{2+} sensitivity that are poorly coupled to Ca^{2+} sparks (18, 20). These mice are also HT. Thus, downregulation of the $\beta 1$ subunit may underlie the changes in BK channel function observed during hypertension. We used functional and molecular approaches to test this hypothesis.

In addition to enhancing Ca^{2+} sensitivity, the $\beta 1$ subunit modifies gating and pharmacologic features of BK channels. In the presence of the $\beta 1$ subunit, open dwell times of single BK channels are increased (29). If $\beta 1$ expression is decreased in HT arterial myocytes, as suggested by the decrease in Ca^{2+} sensitivity, then one would expect that the BK channel open times should be decreased. To test this, we examined the open times of BK channels in NT and HT myocytes by constructing open time histograms at a membrane potential of $+40$ mV with a free Ca^{2+} of $1 \mu\text{M}$. Figure 3b shows representative single-channel recordings and respective open time histograms from NT and HT myocytes. Clearly, the open dwell times of HT BK channels are decreased relative to those of BK channels from NT arteries (9.9 ± 1.5

ms vs. 18.0 ± 2.7 ms, $P < 0.05$, $n = 9$ patches each), which is consistent with decreased expression of the $\beta 1$ subunit of the BK channel in HT arteries.

The $\beta 1$ subunit also confers sensitivity to acute activation of BK channels by estradiol (30) and the xenoestrogen tamoxifen (31). If the $\beta 1$ subunit is downregulated as suggested by the observed decrease in BK channel open time and Ca^{2+} sensitivity, then BK channels should be less sensitive to acute activation by tamoxifen (Tam). Therefore, we used Tam as a pharmacologic probe to assess $\beta 1$ subunit function in NT and HT arterial myocytes. We examined the Tam sensitivity of BK channels in excised patches at a membrane potential of +40 mV with 100-nM free Ca^{2+} . Tam exposure (Figure 3c) increased the P_o of BK channels from NT myocytes (4.0 ± 1.2 -fold), whereas those from HT myocytes were minimally affected (1.5 ± 0.5 -fold; $P < 0.05$, $n = 5$ patches each). Reduction of BK single-channel conductance by Tam resides in the pore-forming α subunit (31). Although the effect of Tam on P_o was primarily limited to NT BK channels, Tam produced the same reduction in BK single-channel current amplitude in NT ($7.0\% \pm 0.9\%$) and HT ($6.8\% \pm 0.7\%$) patches (Figure 3c; $P > 0.05$, $n = 5$ each). Thus, the reduced effect of Tam on BK channel P_o in HT patches did not result from the lack of Tam-BK channel interaction. From these results (decreased coupling of BK channels from Ca^{2+} sparks, reduced BK channel Ca^{2+} sensitivity, decreased open dwell time, and decreased sensitivity to activation by Tam), we conclude that, in comparison with NT arteries, $\beta 1$ subunit function is reduced in HT arterial myocytes.

Downregulation of $\beta 1$, but not α , mRNA during hypertension. To address the origin of the apparent reduction in $\beta 1$ subunit function observed in HT arteries, we examined $\beta 1$ expression at the transcriptional level by conventional RT-PCR. In these experiments, we also examined the expression the pore-forming α subunit, which has been suggested to be upregulated in other models of hypertension (32). Figure 4a demonstrates a clear reduction in the amplification of $\beta 1$ transcripts with no obvious change in the α signal. To confirm these findings, we used real-time RT-PCR to determine the relative abundance (normalized to 18S RNA) of α and $\beta 1$ transcripts in NT and HT arteries. Real-time RT-PCR demonstrated that in NT arteries, the relative abundance of α and $\beta 1$ transcript was equal (Figure 4b; $P > 0.05$, $n = 3$ animals). In HT arteries, pore-forming α transcripts were not different from NT arteries (Figure 4b; $P > 0.05$, $n = 3$ animals), whereas $\beta 1$ transcripts were approximately 65% less abundant than in NT arteries (Figure 4b; $P < 0.05$, $n = 3$ animals). These results are consistent with the apparent decrease in $\beta 1$ subunit function and the lack of difference in BK channel density in excised membrane patches (see Figure 3). We conclude that the decrease in BK channel activity observed in HT arteries, including the apparent reduction in $\beta 1$ subunit function, resulted from downregulation of $\beta 1$ gene transcripts.

Discussion

In this study we have presented data supporting the novel hypothesis that during Ang II-induced hypertension, downregulation of the BK channel $\beta 1$ subunit results in BK channels with reduced open conformation stability and with lower sensitivity to physiologically relevant changes in $[\text{Ca}^{2+}]_i$. The implications of our findings are profound. First, changes in the stoichiometric composition of BK channel subunits can occur during pathologic conditions such as hypertension. Indeed, these findings raise the intriguing possibility of differential regulation of BK channel subunit expression as a mechanism for the control of vascular function. Second, decreasing expression of the $\beta 1$ subunit dramatically reduces the ability of Ca^{2+} sparks to activate BK channels and compromises the ability of the artery to oppose increased contractile stimuli during hypertension. Third, decreased $\beta 1$ function during hypertension diminishes the possibility of acute modulation of BK channels by estrogen (30).

The mechanisms by which a reduction in BK channel function may lead to increased vasoconstriction have been examined by a series of recent studies. It has been proposed that inhibition of BK channels with Ibtx (23) or inhibition of their physiologic activators, Ca^{2+} sparks (9), results in vascular smooth muscle depolarization thereby increasing the opening of voltage-activated L-type Ca^{2+} channels. The resulting increase in Ca^{2+} influx raises global $[\text{Ca}^{2+}]_i$, which causes vasoconstriction and hence contributes to increased

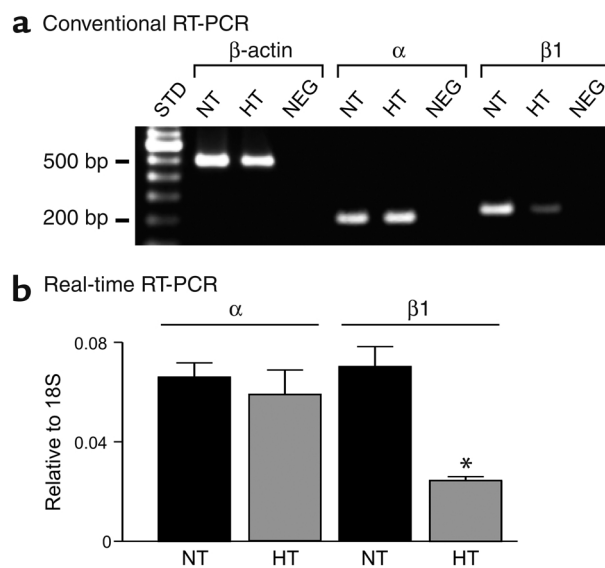


Figure 4 The mRNA levels of $\beta 1$, but not α , are downregulated in HT cerebral arteries. (a) Conventional RT-PCR analysis of α and $\beta 1$ transcript expression in NT and HT arteries. STD = 100-bp marker; NEG = non-template control. (b) Bar plot of the α and $\beta 1$ transcript abundance in NT and HT smooth muscle as determined by real-time RT-PCR. For each sample, α and $\beta 1$ amplifications were normalized to the amount of 18S RNA present. See the Methods section for all primer and probe sequences. * $P < 0.05$.

arterial pressure. It is important to note that expression of L-type Ca^{2+} channels is reportedly higher in vascular smooth muscle cells of HT than in NT animals (33–35). Thus, membrane depolarization, together with an increase in voltage-activated Ca^{2+} channel number, could conspire to produce a large increase in global $[\text{Ca}^{2+}]_i$ and vasoconstriction.

This is the first study to examine the role of RyR-BK channel communication and the subunit composition of BK channels in HT vascular smooth muscle. However, the Ca^{2+} sensitivity of single BK channels in smooth muscle of cerebral arteries and the aorta from spontaneously hypertensive rats (SHR), a genetic model of hypertension, has been previously investigated (32, 36). These studies examined the activity of BK channels from SHR and Wistar Kyoto rats (WKY), the animals regularly used as a control for SHR. Smooth muscle cells isolated from these animals were used to record the activity of single BK channels at Ca^{2+} concentrations ranging from 0.1 to 10 μM . In contrast to our findings, these authors (32, 36) found an increased number of BK channels in smooth muscle cells from SHR rats compared with WKY rats. Furthermore, they found no difference in the ability of BK channels to respond to changes in $[\text{Ca}^{2+}]_i$. Because hypertension is a heterogeneous polygenic disorder, differences between genetic and acquired models of hypertension are not surprising (37). However, it is important that future studies examine $\beta 1$ expression in SHR and WKY rats.

At present, the molecular mechanisms underlying downregulation of the $\beta 1$ subunit in HT rats are unclear. One intriguing possibility is that an increase in Ang II signaling could lead to $\beta 1$ downregulation. Although Ang II levels in NT and HT subjects may be comparable (38), it is important to note that in humans, an Ang I receptor polymorphism with enhanced responsiveness to Ang II (39) has been associated with essential hypertension (40). Thus, renin-Ang activity may be increased during hypertension even in the absence of elevated Ang II plasma levels. Future experiments will address the nature of the renin-Ang system regulation of $\beta 1$ expression in vascular smooth muscle.

Our data clearly demonstrate that the molecular composition of BK channels is altered during hypertension. However, the exact subunit stoichiometry of BK channels in HT vascular smooth muscle cells is presently unclear. Comparison of the data shown in Figure 3 with that obtained by Brenner et al. (18) using $\beta 1$ KO mice may provide some insight. We found that at -40 mV and 10 μM Ca^{2+} , the P_o of BK channels in HT cells was about 0.25 (compared with about 0.50 in NT cells). This P_o is significantly larger than the value reported ($P_o < 0.01$) by Brenner et al. (18) from $\beta 1$ KO cells under similar experimental conditions. Assuming that mouse and rat BK channels have similar voltage and Ca^{2+} dependencies, our data suggest that not all BK channels in HT smooth muscle cells are devoid of $\beta 1$. Future experiments will examine the exact subunit stoichiometry of BK channels in NT and HT vascular smooth muscle cells.

We found that Ca^{2+} spark activity was not depressed in smooth muscle cells from HT, Ang II-infused animals. Ca^{2+} spark amplitude and duration were actually greater in isolated HT smooth muscle cells (see Figure 2). However, in vivo activation of PKC by Ang II could inhibit Ca^{2+} sparks, thus decreasing BK channel activity (11). PKC could also inhibit voltage-gated, delayed-rectifier K^+ channels (41). Thus, increased Ang II signaling could depolarize and thereby constrict vascular smooth muscle by inhibiting Ca^{2+} sparks, reducing $\beta 1$ expression and/or inhibiting voltage-gated, delayed-rectifier K^+ currents.

To conclude, the results of this study suggest a novel mechanism underlying smooth muscle dysfunction during hypertension. Our findings raise the intriguing possibility that downregulation of the $\beta 1$ subunit may be an active component in the natural development of hypertension. Finally, this study indicates that increasing the sensitivity of BK channels to Ca^{2+} , either by restoring $\beta 1$ function or by increasing the intrinsic Ca^{2+} sensitivity of the α subunit, may be a therapeutic approach to correcting vascular dysfunction during hypertension.

Acknowledgments

We thank Stephen M. Schwartz and Patti Polinsky for help with implanting osmotic minipumps and performing blood pressure measurements. We also thank Rachel Grevin for technical assistance and Scott Votaw for help with image analysis. We are also grateful to Bertil Hille and Carmen A. Ufret and Eric G. Chase for critically reading this manuscript. This work was supported by National Institute of Neurological Disease and Stroke grant NS34905 to L.F. Santana and M.T. Nelson. Support for this study was also provided by the Totman Medical Research Trust Fund and grants HL44455 and HL63722 to M.T. Nelson.

1. MacMahon, S., et al. 1990. Blood pressure, stroke, and coronary heart disease. Part 1. Prolonged differences in blood pressure: prospective observational studies corrected for the regression dilution bias. *Lancet*. **335**:765–774.
2. He, J., and Whelton, P.K. 1999. Elevated systolic blood pressure and risk of cardiovascular and renal disease: overview of evidence from observational epidemiologic studies and randomized controlled trials. *Am. Heart J.* **138**:211–219.
3. Folkow, B. 1982. Physiological aspects of primary hypertension. *Physiol. Rev.* **62**:347–504.
4. Dunn, W.R., Wallis, S.J., and Gardiner, S.M. 1998. Remodelling and enhanced myogenic tone in cerebral resistance arteries isolated from genetically hypertensive Brattleboro rats. *J. Vasc. Res.* **35**:18–26.
5. Harder, D.R., Smeda, J., and Lombard, J. 1985. Enhanced myogenic depolarization in hypertensive cerebral arterial muscle. *Circ. Res.* **57**:319–322.
6. Wellman, G.C., et al. 2001. Membrane depolarization, elevated Ca^{2+} entry, and gene expression in cerebral arteries of hypertensive rats. *Am. J. Physiol.* **281**:2559–2567.
7. Harder, D.R. 1984. Pressure-dependent membrane depolarization in cat middle cerebral artery. *Circ. Res.* **55**:197–202.
8. Knot, H.J., and Nelson, M.T. 1998. Regulation of arterial diameter and wall $[\text{Ca}^{2+}]_i$ in cerebral arteries of rat by membrane potential and intravascular pressure. *J. Physiol.* **508**:199–209.
9. Nelson, M.T., et al. 1995. Relaxation of arterial smooth muscle by calcium sparks. *Science*. **270**:633–637.
10. Perez, G.J., Bonev, A.D., Patlak, J.B., and Nelson, M.T. 1999. Functional coupling of ryanodine receptors to K_{Ca} channels in smooth muscle cells from rat cerebral arteries. *J. Gen. Physiol.* **113**:229–238.

11. Bonev, A.D., Jaggar, J.H., Rubart, M., and Nelson, M.T. 1997. Activators of protein kinase C decrease Ca^{2+} spark frequency in smooth muscle cells from cerebral arteries. *Am. J. Physiol.* **273**:2090-2095.
12. Porter, V.A., et al. 1998. Frequency modulation of Ca^{2+} sparks is involved in regulation of arterial diameter by cyclic nucleotides. *Am. J. Physiol.* **274**:1346-1355.
13. Jaggar, J.H., et al. 2002. Carbon monoxide dilates cerebral arterioles by enhancing the coupling of Ca^{2+} sparks to Ca^{2+} -activated K^+ channels. *Circ. Res.* **91**:610-617.
14. Knaus, H.G., Garcia-Calvo, M., Kaczorowski, G.J., and Garcia, M.L. 1994. Subunit composition of the high conductance calcium-activated potassium channel from smooth muscle, a representative of the *mSlo* and *slowpoke* family of potassium channels. *J. Biol. Chem.* **269**:3921-3924.
15. Tanaka, Y., Meera, P., Song, M., Knaus, H.G., and Toro, L. 1997. Molecular constituents of maxi K_{Ca} channels in human coronary smooth muscle: predominant $\alpha + \beta$ subunit complexes. *J. Physiol.* **502**:545-557.
16. Cox, D.H., and Aldrich, R.W. 2000. Role of the $\beta 1$ subunit in large-conductance Ca^{2+} -activated K^+ channel gating energetics. Mechanisms of enhanced Ca^{2+} sensitivity. *J. Gen. Physiol.* **116**:411-432.
17. Meera, P., Wallner, M., Jiang, Z., and Toro, L. 1996. A calcium switch for the functional coupling between alpha (*hSlo*) and β subunits (Kv, $Ca\beta$) of maxi K channels. *FEBS Lett.* **385**:127-128.
18. Brenner, R., et al. 2000. Vasoregulation by the $\beta 1$ subunit of the calcium-activated potassium channel. *Nature.* **407**:870-876.
19. Lohn, M., et al. 2001. $\beta 1$ -Subunit of BK channels regulates arterial wall $[Ca^{2+}]$ and diameter in mouse cerebral arteries. *J. Appl. Physiol.* **91**:1350-1354.
20. Plugger, S., et al. 2000. Mice with disrupted BK channel $\beta 1$ subunit gene feature abnormal Ca^{2+} spark/STOC coupling and elevated blood pressure. *Circ. Res.* **87**:53-60.
21. Wiener, J., Lombardi, D.M., Su, J.E., and Schwartz, S.M. 1996. Immunohistochemical and molecular characterization of the differential response of the rat mesenteric microvasculature to angiotensin-II infusion. *J. Vasc. Res.* **33**:195-208.
22. Cheng, H., et al. 1999. Amplitude distribution of calcium sparks in confocal images: theory and studies with an automatic detection method. *Biophys. J.* **76**:606-617.
23. Brayden, J.E., and Nelson, M.T. 1992. Regulation of arterial tone by activation of calcium-dependent potassium channels. *Science.* **256**:532-535.
24. Knot, H.J., Standen, N.B., and Nelson, M.T. 1998. Ryanodine receptors regulate arterial diameter and wall Ca^{2+} in cerebral arteries of rat via Ca^{2+} -dependent K^+ channels. *J. Physiol.* **508**:211-221.
25. Galvez, A., et al. 1990. Purification and characterization of a unique, potent, peptidyl probe for the high conductance calcium-activated potassium channel from venom of the scorpion *Buthus tamulus*. *J. Biol. Chem.* **265**:11083-11090.
26. Piskorowski, R., and Aldrich, R.W. 2002. Calcium activation of BK_{Ca} potassium channels lacking the calcium bowl and RCK domains. *Nature.* **420**:499-502.
27. McManus, O.B., et al. 1995. Functional role of the β subunit of high conductance calcium-activated potassium channels. *Neuron.* **14**:645-650.
28. Dworetzky, S.I., et al. 1996. Phenotypic alteration of a human BK (*hSlo*) channel by *hSlobeta* subunit coexpression: changes in blocker sensitivity, activation/relaxation and inactivation kinetics, and protein kinase A modulation. *J. Neurosci.* **16**:4543-4550.
29. Nimigean, C.M., and Magleby, K.L. 1999. The β subunit increases the Ca^{2+} sensitivity of large conductance Ca^{2+} -activated potassium channels by retaining the gating in the bursting states. *J. Gen. Physiol.* **113**:425-440.
30. Valverde, M.A., et al. 1999. Acute activation of Maxi-K channels (*hSlo*) by estradiol binding to the β subunit. *Science.* **285**:1929-1931.
31. Dick, G.M., Rossow, C.F., Smirnov, S., Horowitz, B., and Sanders, K.M. 2001. Tamoxifen activates smooth muscle BK channels through the regulatory $\beta 1$ subunit. *J. Biol. Chem.* **276**:34594-34599.
32. Liu, Y., Hudetz, A.G., Knaus, H.G., and Rusch, N.J. 1998. Increased expression of Ca^{2+} -sensitive K^+ channels in the cerebral microcirculation of genetically hypertensive rats: evidence for their protection against cerebral vasospasm. *Circ. Res.* **82**:729-737.
33. Pratt, P.F., Bonnet, S., Ludwig, L.M., Bonnet, P., and Rusch, N.J. 2002. Upregulation of L-type Ca^{2+} channels in mesenteric and skeletal arteries of SHR. *Hypertension.* **40**:214-219.
34. Rusch, N.J., and Hermsmeyer, K. 1988. Calcium currents are altered in the vascular muscle cell membrane of spontaneously hypertensive rats. *Circ. Res.* **63**:997-1002.
35. Cox, R.H., and Lozinskaya, I.M. 1995. Augmented calcium currents in mesenteric artery branches of the spontaneously hypertensive rat. *Hypertension.* **26**:1060-1064.
36. England, S.K., Wooldridge, T.A., Stekiel, W.J., and Rusch, N.J. 1993. Enhanced single-channel K^+ current in arterial membranes from genetically hypertensive rats. *Am. J. Physiol.* **264**:1337-1345.
37. Sharma, P., et al. 2000. A genome-wide search for susceptibility loci to human essential hypertension. *Hypertension.* **35**:1291-1296.
38. Sim, M.K., and Qui, X.S. 2003. Angiotensins in plasma of hypertensive rats and human. *Regul. Pept.* **111**:179-182.
39. van Geel, P.P., et al. 2000. Angiotensin II type 1 receptor A1166C gene polymorphism is associated with an increased response to angiotensin II in human arteries. *Hypertension.* **35**:717-721.
40. Wang, W.Y., Zee, R.Y., and Morris, B.J. 1997. Association of angiotensin II type 1 receptor gene polymorphism with essential hypertension. *Clin. Genet.* **51**:31-34.
41. Hayabuchi, Y., Standen, N.B., and Davies, N.W. 2001. Angiotensin II inhibits and alters kinetics of voltage-gated K^+ channels of rat arterial smooth muscle. *Am. J. Physiol.* **281**:2480-2489.